

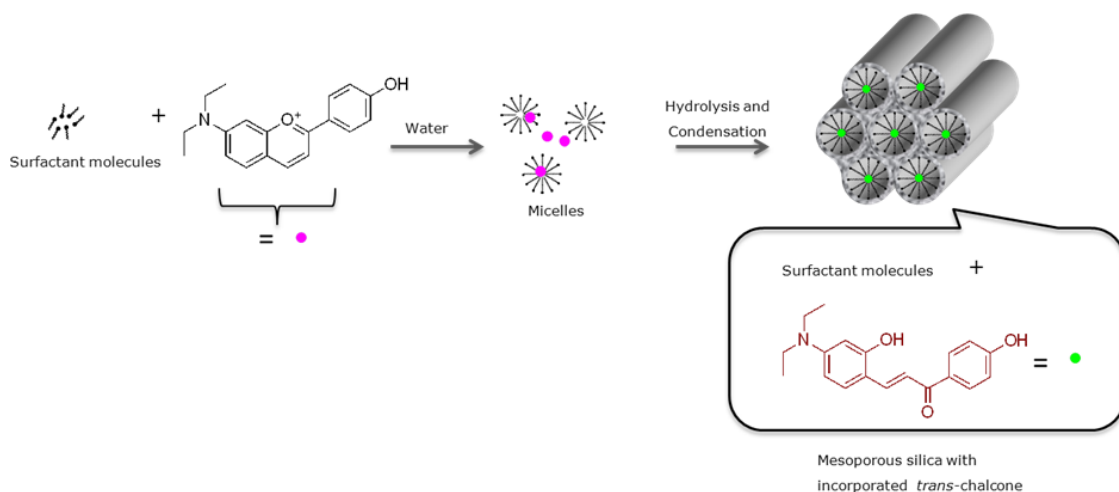
Electronic Supporting Information

pH tunable fluorescence and photochromism of a flavylium-based MCM-41 pigment

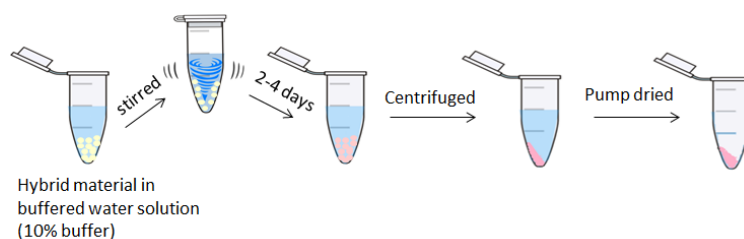
Sandra Gago, Márcia Pessêgo, César A.T. Laia,* A. Jorge Parola*

LAQV-REQUIMTE, Chemistry Department, Faculty of Science and Technology, Universidade

NOVA de Lisboa, 2829-516 Caparica, Portugal. E-Mail: ajp@fct.unl.pt



Scheme S1 – Schematic illustration for the synthesis of MCM-41-Ct powders.



Scheme S2 – Schematic illustration for the pH adjustment of MCM-41-Ct powders.

CHARACTERIZATION

The X-ray powder diffractogram shows four well defined basal reflections indexed to a hexagonal cell and typical of MCM-41 materials (Figure S1).¹ The hexagonal structure parameter a_0 , which is the center to center distance between adjacent pores, was calculated from the main basal reflection (100) ($a_0 = 2d_{100}/\sqrt{3}$), giving $a_0=4.90$ nm ($d_{100}=4.24$ nm). For comparison one sample of MCM-41 was prepared by the same method but without the dye and a similar diffractogram for the non-calcined material with $a_0=4.76$ nm was obtained.

The nitrogen adsorption isotherm reveals low values of BET specific surface area, $13 \text{ m}^2/\text{g}$, and of total pore volume, $0.03 \text{ cm}^3/\text{g}$ which corroborates that the pores are not accessible to the nitrogen adsorbate due to their filling with surfactant molecules. For sample of non-calcined MCM-41 without the dye a BET specific surface area of $6 \text{ m}^2/\text{g}$ was obtained.

The thermogravimetric curve displays three main mass loss regions (Figure S2), the first one that takes place up to $130 \text{ }^\circ\text{C}$ is due to the physically adsorbed water and is about 4%. The major step of weight loss, approximately 38%, occurs in the range of $130 - 300 \text{ }^\circ\text{C}$ and corresponds to the decomposition of the surfactant and of the organic guests molecules. An additional step up to $520 \text{ }^\circ\text{C}$ with a mass loss of 6% is normally attributed to the dehydroxylation of silanols groups.² TEM images show the typical "honeycomb" arrangement of the cylindrical pores of MCM-41 (Figure S3).

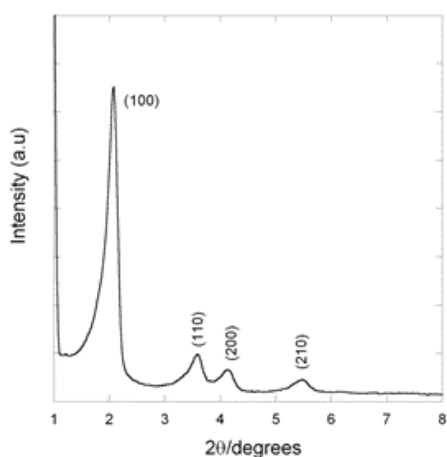


Figure S1 - Powder XRD pattern of MCM-41-Ct.

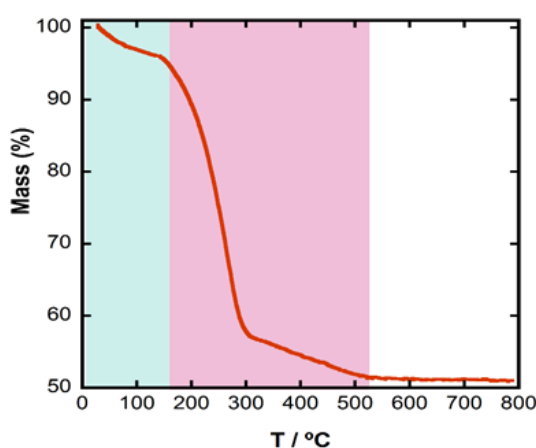


Figure S2 - TGA curve of MCM-41-Ct. TGA curve exhibits two main weight loss regions: up to $140 \text{ }^\circ\text{C}$ - corresponding to the removal of adsorbed water, *ca.* 4%; $140 \text{ }^\circ\text{C} - 500 \text{ }^\circ\text{C}$ - removal of organic molecules, *ca.* 45%; TGA residue - 51%.

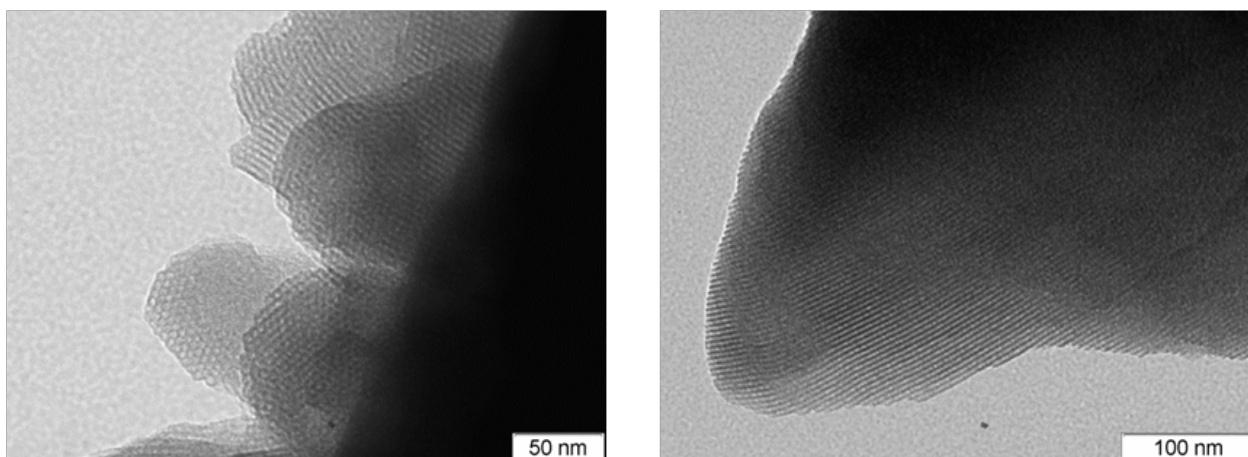


Figure S3 - Transmission Electron Microscopy (TEM) images of MCM-41-Ct.

LUMINESCENCE MEASUREMENTS

Figure S4 shows the excitation/emission mapping of the pigments equilibrated at different pH values. For pH=1, AH^+ species are present and the luminescence properties shows well defined spots with small dependences of emission spectra with excitation wavelength. At pH=7 and 10, ionized Ct species are prevalent and some excitation wavelength dependence is observed probably due to the acid-base equilibria between Ct^- and Ct^{2-} . Fig. S5 shows the fluorescence decays for the three cases. The decays were fitted with the sum of 3 exponentials at pH=7 and 10, while at pH=1 it is a single-exponential followed by a long decay (above 100 ns) probably due to traces of Ct species in the powder.

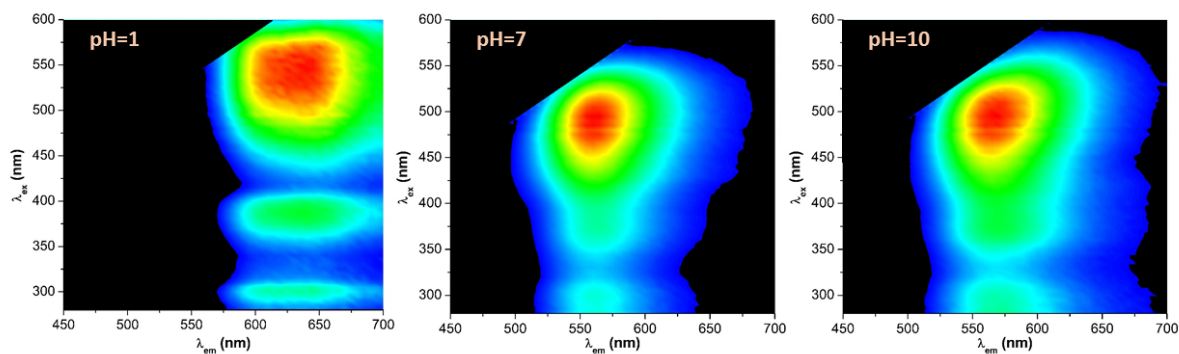


Figure S4 -2D mapping of the fluorescence properties of MCM-41- pigments equilibrated at different pHs.

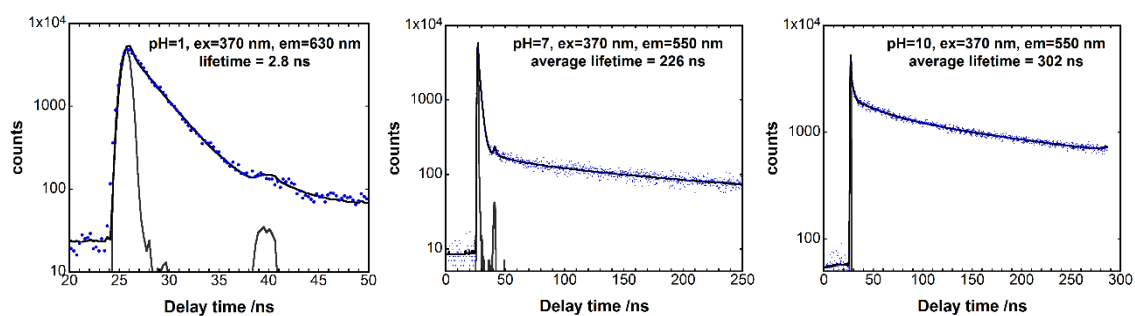


Figure S5 - Fluorescence decays of MCM-41- pigments equilibrated at different pHs. The total counts at the maximum were 5000.

IRRADIATION MEASUREMENTS

Photochromism was observed in the pH range between 2.5 and 4.8. At higher pH the chromic effect became less pronounced, showing nevertheless a shift of the spectra of about 22 nm. This is attributed to the formation of quinoidal base species (**A**) instead of AH^+ where the effect is more significant (Figure S6).

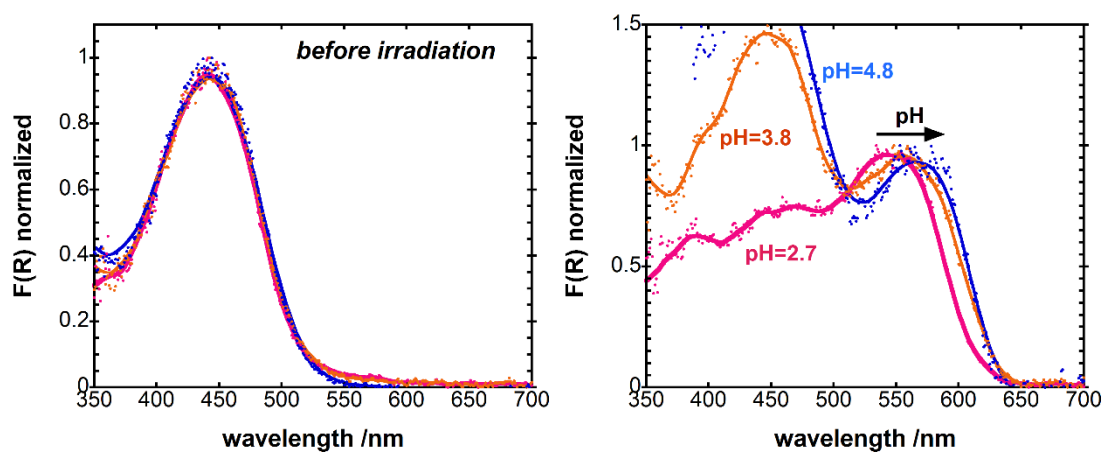


Figure S6 - Normalized absorption spectra of MCM-41-Ct pigments equilibrated at different pH before and after irradiation ($\lambda_{\text{irr}}=445 \text{ nm}$ and $I_0=7.53 \times 10^{-8} \text{ Einstein} \cdot \text{min}^{-1}$).

LIXIVIATION DURING pH ADJUSTMENT

During pH adjustment there is so lixiviation of the dye from the MCM-41 particles (Fig. S7). Taking into account the absorption spectra of the supernatant, the loss of dye is less than 10% until about pH=5 (at pH=4.8 it is 8.3%). Then by decreasing pH the lixiviation becomes more pronounced, being about 25% at pH=3.6 and 50% at pH=1.6. This shows that only at rather low pH it becomes an important effect during the pH adjustment.

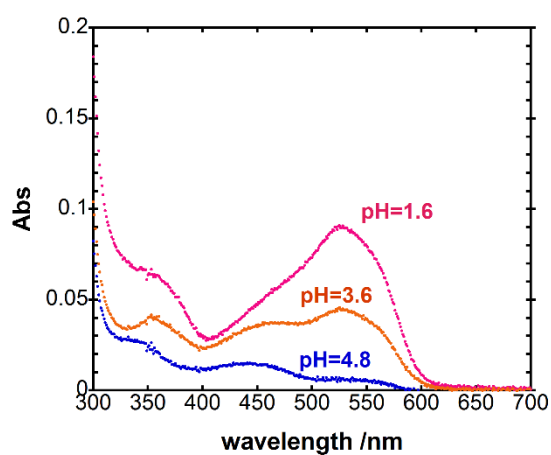


Figure S7 - Supernatant absorption spectra after pH adjustment of MCM-41 pigments

THERMAL RECOVERY

The thermal recovery of the pigment was measured using the conditions described on Figure 3 and 4. Fig. S8 shows the data to calculate the recovery data to calculate the $t_{1/2}$ of the process.

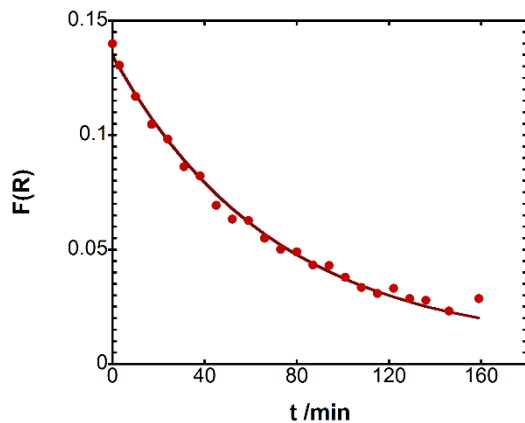


Figure S8 - Recovery cycles of MCM-41-Ct pigment (pH=2.7) monitored at 550 nm following the same experimental details described in Figure 3. The data is fitted with single-exponential kinetics.

References

- (1) Beck, J. S.; Vartuli, J. C.; Roth, W. J.; Leonowicz, W. J.; Kresge, C. T.; Schmitt, K. D.; Chu, C. T. W.; Olson, D. H.; Sheppard, E. W.; McCullen, S. B.; Higgins, J. B.; Schlenker, J. L. A new family of mesoporous molecular sieves prepared with liquid crystal templates. *J. Am. Chem. Soc.*, **1992**, *114*, 10834–10843.
- (2) Zhao, X. S. ; Lu, G. Q.; Whittaker, A. K.; Millar, G. J.; Zhu, H. Y. Comprehensive Study of Surface Chemistry of MCM-41 Using ^{29}Si CP/MAS NMR, FTIR, Pyridine-TPD, and TGA. *J. Phys. Chem. B*, **1997**, *101*, 6525-6531.